

## Neutron and proton matrix elements for $2_1^+$ transitions in $T = 1$ nuclei from pion inelastic scattering

C. L. Morris

*Los Alamos National Laboratory, Los Alamos, New Mexico 87545*

S. J. Seestrom-Morris,\* D. Dehnhard, and C. L. Blilie<sup>†</sup>

*University of Minnesota, Minneapolis, Minnesota 55455*

R. Gilman,<sup>‡</sup> G. P. Gilfoyle,<sup>§</sup> J. D. Zumbro, M. G. Burlein, S. Mordechai,\*\* and H. T. Fortune

*University of Pennsylvania, Philadelphia, Pennsylvania 19104*

L. C. Bland,<sup>††</sup> M. Brown, D. P. Saunders,<sup>‡‡</sup> P. A. Seidl,<sup>§§</sup> and C. Fred Moore

*University of Texas at Austin, Austin, Texas 78712*

K. Maeda

*Tohoku University, Sendai, Japan*

G. S. Blanpied

*University of South Carolina, Columbia, South Carolina 29208*

B. A. Brown

*Michigan State University, East Lansing, Michigan 48824*

(Received 17 November 1986)

Cross sections have been measured for  $\pi^+$  and  $\pi^-$  inelastic scattering to the  $2_1^+$  levels of  $^{18}\text{O}$ ,  $^{22}\text{Ne}$ ,  $^{26}\text{Mg}$ ,  $^{30}\text{Si}$ , and  $^{34}\text{S}$ . The data are used to infer neutron and proton quadrupole-matrix elements for these transitions. The matrix elements extracted from the pion data are in good agreement with their corresponding electromagnetic matrix elements. These results indicate that the use of the distorted-wave impulse approximation is a valid procedure for this class of transition.

Comparisons of  $\pi^+$  and  $\pi^-$  inelastic scattering in the region of the pion nucleon  $\Delta_{3/2,3/2}$  (1232 MeV) resonance are ideal for determining the relative contributions of neutrons and protons to inelastic transitions.<sup>1</sup> Under the assumption of charge symmetry, the neutron matrix element  $M_n$  ( $T_z = T$ ), measured for a transition in a nucleus with its  $z$  component of isospin  $T_z$  equal to the total isospin  $T$ , is equal to the electromagnetic matrix element  $M_p$  ( $T_z = -T$ ) in the mirror nucleus. We can test models of the pion-nucleus interaction by comparing  $M_n(+1)$  extracted from pion scattering with  $M_p(-1)$  obtained from the lifetime measurements<sup>2</sup> that have already been measured for many  $2_1^+ \rightarrow 0_1^+$  transitions in  $T_z = -1$   $sd$ -shell nuclei.

Cross sections have been measured previously for  $\pi^\pm$  inelastic scattering near the  $\Delta_{3/2,3/2}$  ( $T_\pi \approx 180$  MeV) to the  $2_1^+$  states in  $^{18}\text{O}$ ,<sup>3,4</sup>  $^{26}\text{Mg}$ ,<sup>5</sup> and  $^{42}\text{Ca}$ .<sup>6</sup> Low energy ( $T_\pi = 50$  MeV) cross sections have been measured for the  $2_1^+$  states in  $^{26}\text{Mg}$  (Ref. 7) and  $^{34}\text{S}$ .<sup>8</sup> Although matrix-element ratios  $M_n(+1)/M_p(+1)$  extracted from pion data are generally in agreement with the ratios  $M_p(-1)/M_p(+1)$  obtained with electromagnetic probes,<sup>9,10</sup> the models used in the analysis of the pion data have not been consistent and the precision of these comparisons has been poor.

In this paper we report new data and an analysis of cross sections for  $\pi^+$  and  $\pi^-$  inelastic scattering to the  $2_1^+$  levels in the nuclei  $^{18}\text{O}$ ,  $^{22}\text{Ne}$ ,  $^{26}\text{Mg}$ ,  $^{30}\text{Si}$ , and  $^{34}\text{S}$ . The data were obtained using the Energetic Pion Channel and Spectrometer at the Clinton P. Anderson Meson Physics Facility. Cross sections for  $^{18}\text{O}$  and  $^{22}\text{Ne}$  were measured using a cooled-gas target.<sup>11</sup> Data for all the solid targets were measured simultaneously using strip targets mounted in the incident pion beam. Angular distributions were measured for all targets between  $\theta_{\text{lab}} = 20^\circ$  and  $40^\circ$  at an incident pion energy of 180 MeV. Typical spectra are shown in Fig. 1.

Absolute normalizations were determined by comparing  $\pi$ -p yields to  $\pi$ -p cross sections calculated from pion-nucleon phase shifts.<sup>12</sup> For the gas target,  $\pi$ -p yields were measured by scattering from methane ( $\text{CH}_4$ ) gas. The  $\pi$ -p yields for the solid target data were measured by using a solid polyethylene ( $\text{CH}_2$ ) target. The relative normalization between  $\pi^+$  and  $\pi^-$  is known to better than  $\pm 3\%$  and the absolute normalization is known to  $\pm 10\%$ .

We analyzed the data by comparing them with distorted-wave impulse-approximation (DWIA) calculations performed using the code DWPI.<sup>13</sup> We used the Kisslinger<sup>14</sup> form for the optical potential with parameters previously determined by Boyer *et al.*<sup>6</sup> The DWIA

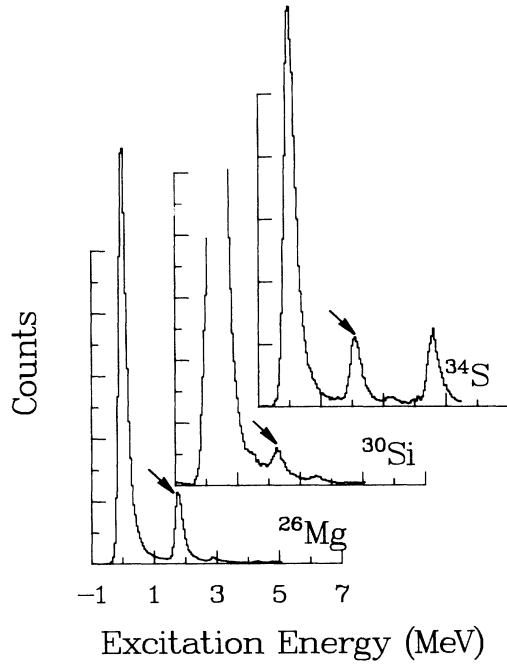


FIG. 1. Spectra obtained for  $\pi^+$  scattering from  $^{26}\text{Mg}$ ,  $^{30}\text{Si}$ , and  $^{34}\text{S}$ .

calculations were simultaneously fitted to the  $\pi^+$  and  $\pi^-$  data by adjusting the proton and neutron deformation parameters  $\beta_p$  and  $\beta_n$ . The resulting transition densities were integrated to obtain matrix elements,

$$M_i \equiv e \int_0^\infty r^{l+2} \rho_{\text{tr},i}(r) dr \quad (i = p, n), \quad (1)$$

with

$$\rho_{\text{tr},i}(r) = -\beta_i R_i \frac{d\rho_i(r)}{dr} \quad \text{and } l = 2, \quad (2)$$

where  $l$  is the multipolarity of the transition,  $\rho_{\text{tr},i}$  is the proton or neutron transition density, and  $\rho_i$  is the proton or neutron ground-state density, with half-density radius  $R_i$ . The reduced transition probability [ $B(E2\uparrow)$ ] from

the  $0^+$  ground state to the  $2^+$  state is given by  $B(E2\uparrow) = M_p^2$ .

Because of the neutron excess in these nuclei, there may be differences between the neutron and proton ground-state distributions that could influence our analysis. To account for this, we have fitted two-parameter Fermi functions,

$$\rho(r) = \rho_0 \{1 + \exp[(r - R_1)/a_i]\}^{-1},$$

to Hartree-Fock ground state densities of the Skyrme III interaction.<sup>15</sup> The rms radius of each fitted density was constrained to be the same as that of the corresponding Hartree-Fock density. The resulting parameters are listed in Table I. The fitted point proton rms radii  $\langle r_p^2 \rangle_{\text{fit}}^{1/2}$  and the values  $\langle r_p^2 \rangle_{\text{expt}}^{1/2}$  determined from the measured charge densities are also given in Table I. We find the agreement is good.

The relationship between the matrix elements and the peak cross sections is given approximately by

$$\sigma^+ = K^+ (3M_p + M_n)^2, \quad (3)$$

$$\sigma^- = K^- (M_p + 3M_n)^2, \quad (4)$$

where  $K^+$  and  $K^-$  are obtained from the DWIA calculations; the factor of 3 comes from the assumption that the pion-nucleus interaction is dominated by the  $\pi$ -nucleon  $\Delta_{3/2,3/2}$  resonance.

The solutions of these equations are shown graphically in Fig. 2. There are generally two solutions, one with the neutron and proton amplitudes in phase and one with them out of phase. Because low-lying states in even-even nuclei are expected to be predominantly isoscalar, the solution with the neutron and proton amplitudes in phase has been assumed for all of the transitions presented in the current analysis. Matrix elements were obtained by varying  $\beta_n$  and  $\beta_p$  to give the best fit to the entire range of the angular distribution. The measured and calculated cross-section angular distributions are shown in Fig. 3.

The matrix elements resulting from this analysis are listed in Table I. These are compared with the matrix elements extracted from electromagnetic measurements,<sup>16,17</sup> which are also listed in Table I and displayed in Fig. 4.

TABLE I. Matrix elements and parameters.

Nucleus	$R_n$ (fm)	$a_n$ (fm)	$R_p$ (fm)	$a_p$ (fm)	fit <sup>a</sup>	Expt. <sup>b</sup>	Current analysis		Electromagnetic <sup>c</sup>	
					$\langle r_p^2 \rangle^{1/2}$ (fm)	$\langle r_p^2 \rangle^{1/2}$ (fm)	$M_n(+1)$ ( $e \text{ fm}^2$ )	$M_p(+1)$ ( $e \text{ fm}^2$ )	$M_p(-1)$ ( $e \text{ fm}^2$ )	$M_p(+1)$ ( $e \text{ fm}^2$ )
$^{18}\text{O}$	2.83	0.46	2.77	0.42	2.65	2.65	$13.8 \pm 0.7$	$5.6 \pm 0.6$	$16.1 \pm 0.7$	$6.9 \pm 0.1^d$
$^{22}\text{Ne}$	3.03	0.45	3.10	0.40	2.82	2.83	$18.7 \pm 1.3$	$15.2 \pm 1.0$	$21.0 \pm 4.0$	$15.4 \pm 0.5^c$
$^{26}\text{Mg}$	3.19	0.45	3.16	0.44	2.94	2.89	$15.1 \pm 1.1$	$16.5 \pm 1.0$	$18.8 \pm 0.9$	$17.8 \pm 0.3$
$^{30}\text{Si}$	3.35	0.46	3.34	0.44	3.06	3.01	$17.5 \pm 1.1$	$14.6 \pm 1.0$	$17.4 \pm 0.8$	$14.3 \pm 0.4$
$^{34}\text{S}$	3.47	0.49	3.45	0.48	3.21	3.18	$17.1 \pm 1.1$	$15.5 \pm 1.0$	$15.0 \pm 1.0$	$14.2 \pm 0.5$
$^{42}\text{Ca}^f$	3.46	0.55	3.52	0.55	3.41	3.40	$21.3 \pm 1.4$	$18.5 \pm 1.3$	$28.0 \pm 3.0$	$20.4 \pm 0.3$

<sup>a</sup> We calculated  $\langle r_p^2 \rangle_{\text{fit}}^{1/2}$  using  $\langle r_p^2 \rangle_{\text{fit}} = \frac{3}{5} R_p^2 + \frac{7}{5} \pi^2 a_p^2$ .

<sup>b</sup> Compiled by B. A. Brown *et al.* [J. Phys. G **10**, 1683 (1984)];  $\langle r_p^2 \rangle_{\text{expt}}^{1/2}$  was obtained from the rms charge radius  $\langle r_c^2 \rangle^{1/2}$  by  $\langle r_p^2 \rangle_{\text{expt}}^{1/2} = [\langle r_c^2 \rangle - (0.88)^2]^{1/2}$ .

<sup>c</sup> Reference 17.

<sup>d</sup> G. C. Ball *et al.* [Nucl. Phys. **A377**, 281 (1982)] give  $6.4 \pm 0.1$  as a weighted average of all measurements for  $M_p(+1)$  in  $^{18}\text{O}$ .

<sup>e</sup> Electromagnetic values for  $^{22}\text{Ne}$  are from Ref. 16.

<sup>f</sup> The  $^{42}\text{Ca}$  data are from Ref. 6.

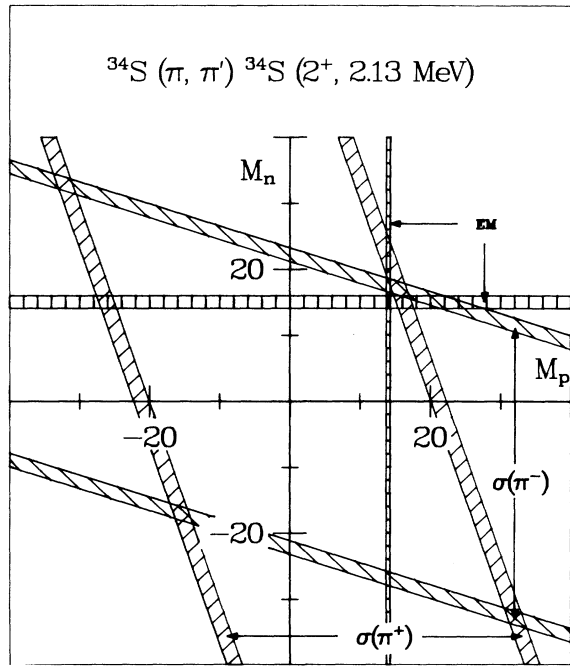


FIG. 2. Graphic solutions of  $M_n$  and  $M_p$ . The bands labeled  $\sigma(\pi^+)$  and  $\sigma(\pi^-)$  represent the values of  $M_n$  and  $M_p$  that are consistent with the  $\pi^+$  or  $\pi^-$  data. The intersections of the two  $\sigma(\pi^+)$  and  $\sigma(\pi^-)$  bands indicate the values of  $M_n$  and  $M_p$  that simultaneously fit the  $\pi^+$  and  $\pi^-$  data.

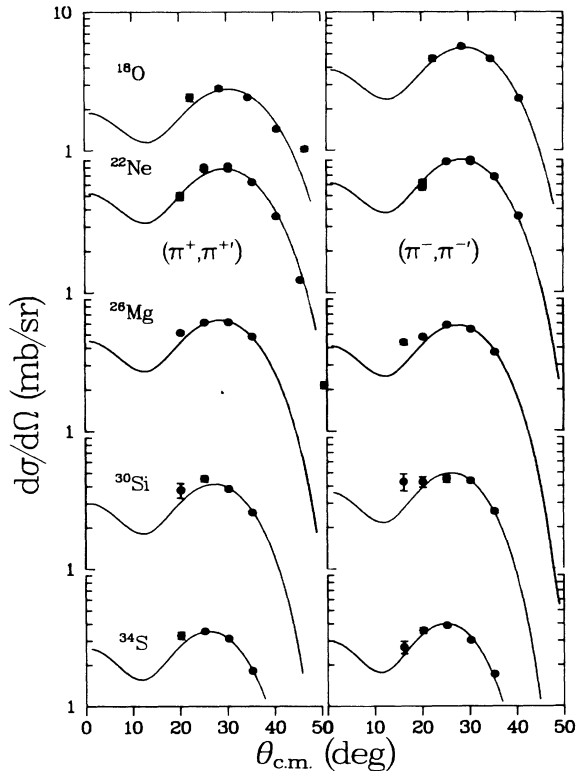


FIG. 3. Angular distributions measured at  $T_\pi=180$  MeV.

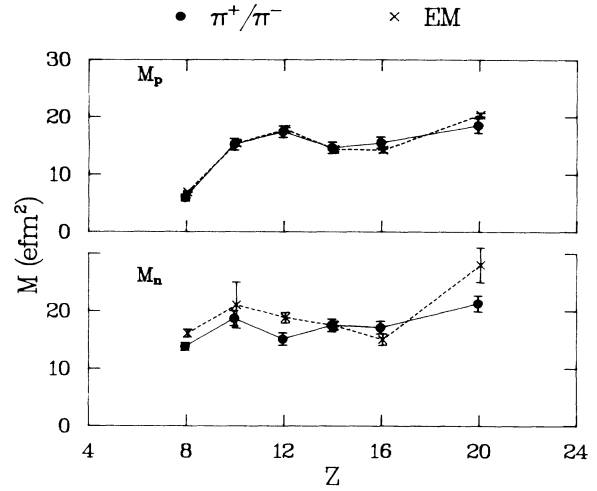


FIG. 4.  $Z$  dependence of the quadrupole-matrix elements  $M_p$  and  $M_n$ , extracted from pion scattering, and of the corresponding electromagnetic matrix elements.

Previously reported results<sup>6</sup> for  $^{42}\text{Ca}$  are also given. The proton matrix elements extracted from the analysis of the pion scattering data agree well with those extracted from lifetime measurements in the target nuclei. We find that the weighted average over all nuclei of the ratio of  $M_p(+1)$  obtained from electromagnetic measurements to that obtained from our analysis is  $1.01 \pm 0.03$ .

There are significant differences between earlier compilations<sup>18</sup> of  $M_p(-1)$  and more recent results.<sup>17</sup> We find better agreement between our neutron matrix elements and the newer proton matrix elements. The value of the ratio of  $M_p(-1)$  from the electromagnetic data<sup>17</sup> to  $M_n(+1)$  from this pion analysis varies from 0.88 for  $^{34}\text{S}$  to 1.31 for  $^{42}\text{Ca}$ ; the weighted average over  $^{18}\text{O}$ ,  $^{22}\text{Ne}$ ,  $^{26}\text{Mg}$ ,  $^{30}\text{Si}$ ,  $^{34}\text{S}$ , and  $^{42}\text{Ca}$  is  $1.08 \pm 0.04$ .

The enhancement in  $M_p(-1)$  from mirror nucleus electromagnetic measurements with respect to  $M_n(+1)$  from pion scattering measurements may be due to the Coulomb force. Coulomb-induced mixing of the isovector giant quadrupole resonance into low-lying states and Coulomb effects on the single-particle wave functions both tend to enhance  $M_p(-1)$  with respect to  $M_n(+1)$ . This enhancement has been estimated<sup>19,20</sup> to be as much as 10%.

The quality of the agreement between the pion results and the electromagnetic measurements is remarkably good in view of recent predictions made by Hirata, Lenz, and Theis.<sup>21</sup> They suggest that the isoscalar part of the pion-nucleus interaction should be quenched by 20–30% and that the isovector part of the interaction should be enhanced by a similar amount due to  $\Delta$ -nucleus interactions. If such a drastic modification of the interaction is used in the current analysis, the matrix elements  $M_n$  and  $M_p$  are increased by about 20–30%. This would destroy the agreement between the electromagnetic and pion results.

In summary, we have observed good agreement between proton quadrupole matrix elements  $M_p(+1)$  extracted

from pion inelastic scattering and those obtained from lifetime measurements, and fair agreement between neutron quadrupole matrix elements  $M_n(+1)$  extracted from pion inelastic scattering and the matrix elements  $M_p(-1)$  obtained from lifetime measurements in the corresponding mirror nuclei. This good agreement lends validity to the

use of the distorted wave impulse approximation in the analysis of resonance-energy pion inelastic scattering.

This work was supported in part by the U.S. Department of Energy, the Robert A. Welch Foundation, and the National Science Foundation.

\*Present address: Los Alamos National Laboratory, Los Alamos, NM 87545.

†Present address: Mission Research Corporation, Santa Barbara, CA 93102.

‡Present address: Physics Division, Argonne National Laboratory, Argonne, IL 60439.

§Present address: State University of New York at Stony Brook, Stony Brook, NY 11794.

\*\*Permanent address: Ben-Gurion University of the Negev, Beer-Sheva, Israel.

††Present address: Indiana University Cyclotron Facility, Bloomington, IN 47405.

‡‡Present address: Air Force Academy, Colorado Springs, CO 80840.

§§Present address: Lawrence Berkeley Laboratory, Berkeley, CA 94720.

<sup>1</sup>C. L. Morris, Phys. Rev. C **13**, 1755 (1976).

<sup>2</sup>A. M. Bernstein, V. R. Brown, and V. A. Madsen, Phys. Lett. **42**, 425 (1979).

<sup>3</sup>S. Iverson, A. Obst, Kamal K. Seth, H. A. Thiessen, C. L. Morris, N. Tanaka, E. Smith, J. F. Amann, R. Boudrie, G. Burleson, M. Devereux, L. W. Swenson, P. Varghese, K. Boyer, W. J. Braithwaite, W. Cottingame, and C. Fred Moore, Phys. Rev. Lett. **40**, 17 (1978).

<sup>4</sup>J. Jansen, J. Zichy, J. P. Albanèse, J. Arvieux, J. Bolger, E. Boschitz, C. H. Q. Ingram, and L. Pflug, Phys. Lett. **77B**, 359 (1978).

<sup>5</sup>C.-A. Wiedner, K. R. Cordell, W. Saathoff, S. T. Thornton, J. Bolger, E. Boschitz, G. Proebstle, and J. Zichy, Phys. Lett. **97B**, 37 (1980).

<sup>6</sup>K. G. Boyer, William B. Cottingame, L. E. Smith, Steven J. Greene, C. Fred Moore, J. S. McCarthy, R. C. Minehart, J. F. Davis, G. R. Burleson, G. Blanpied, Chuck A. Goulding, Henry A. Thiessen, and Christopher L. Morris, Phys. Rev. C

**24**, 598 (1981).

<sup>7</sup>R. Tacik, K. L. Erdman, R. R. Johnson, H. W. Roser, D. R. Gill, E. W. Blackmore, R. J. Sobie, T. E. Drake, S. Martin, and C. A. Wiedner, Phys. Rev. Lett. **52**, 1276 (1983).

<sup>8</sup>R. J. Sobie, T. E. Drake, K. L. Erdman, R. R. Johnson, H. W. Roser, R. Tacik, E. W. Blackmore, D. R. Gill, S. Martin, C.-A. Wiedner, and T. Masterson, Phys. Rev. C **30**, 1612 (1984).

<sup>9</sup>C. L. Morris, Workshop on Nuclear Structure with Intermediate Energy Probes, Los Alamos National Laboratory Report LA-8303-C, p. 57 (1980).

<sup>10</sup>T. K. Alexander, G. C. Ball, W. G. Davis, J. S. Forster, I. V. Mitchell, and H.-B. Mak, Phys. Lett. **113B**, 132 (1982).

<sup>11</sup>C. L. Morris *et al.* (unpublished).

<sup>12</sup>Glenn Rowe, Martin Salomon, and Rubin H. Landau, Phys. Rev. C **18**, 584 (1978).

<sup>13</sup>R. A. Einstein and G. A. Miller, Comput. Phys. Commun. **11**, 95 (1976).

<sup>14</sup>L. S. Kisslinger, Phys. Rev. **98**, 761 (1955).

<sup>15</sup>M. Beiner, H. Flocard, Nguyen Van Giai, and P. Quentin, Nucl. Phys. **A238**, 29 (1975).

<sup>16</sup>P. M. Endt and C. Van Der Leun, Nucl. Phys. **A310**, 1 (1978).

<sup>17</sup>T. K. Alexander, B. Castel, and I. S. Towner, Nucl. Phys. **A445**, 189 (1985).

<sup>18</sup>A. M. Bernstein, R. A. Misskimen, B. Quinn, S. A. Wood, M. V. Hynes, G. S. Blanpied, B. G. Ritchie, and V. R. Brown, Phys. Rev. Lett. **49**, 451 (1982).

<sup>19</sup>B. A. Brown, A. Arima, and J. B. McGrory, Nucl. Phys. **A277**, 77 (1977).

<sup>20</sup>B. A. Brown, B. H. Wildenthal, W. Chung, S. E. Massen, M. Bernas, A. M. Bernstein, R. Miskimen, V. R. Brown, and V. A. Madsen, Phys. Rev. C **26**, 2247 (1982).

<sup>21</sup>M. Hirata, F. Lenz, and M. Thies, Phys. Rev. C **28**, 785 (1983).